

In preparation for: Int J Biochem Cell Biol

2017-08-17; Version 17

Full-length review

**Mitochondrial respiratory control:
a conceptual perspective on coupling states in mitochondrial preparations.**

MITOEAGLE recommendations Part 1

MITOEAGLE Terminology Group

Corresponding author: E. Gnaiger

Contributing co-authors (*alphabetical, to be extended*):

M.G. Alves, D. Ben-Shachar, G.C. Brown, G.R. Buettner, P.M. Coen, J.L. Collins, L. Crisostomo, M.S. Davis, C. Doerrier, E. Elmer, A. Filipovska, P.M. Garcia-Roves, D.K. Harrison, K.T. Hellgren, C.L. Hoppel, J. Iglesias-Gonzalez, P. Jansen-Dürr, B.H. Goodpaster, B.A. Irving, S. Iyer, T. Komlodi, V. Laner, H.K. Lee, H. Lemieux, A.T. Meszaros, N. Moiso, A. Molina, A.L. Moore, A.J. Murray, J. Neuzil, R.K. Porter, K. Nozickova, P.J. Oliveira, K. Renner-Sattler, J. Rohlena, D. Salvadego, L.A. Sazanov, O. Sobotka, R. Stocker, I. Szabo, M. Tanaka, L. Tretter, B. Velika, A.E. Vercesi, Y.H. Wei

Supporting co-authors (*alphabetical*):

R.A. Brown, A.J. Chicco, T. Dias, G. Distefano, H. Dubouchaud, L.F. Garcia-Souza, G. Keppner, A. Krajcova, M. Markova, J. Muntané, D. O'Gorman, C.M. Palmeira, P.X. Petit, K. Siewiera, P. Stankova, Z. Sumbalova

[Mitochondrial respiratory control: MITOEAGLE recommendations 1](#)

Correspondence: E. Gnaiger

*Department of Visceral, Transplant and Thoracic Surgery, D. Swarovski Research
Laboratory, Medical University of Innsbruck, Innrain 66/4, A-6020 Innsbruck, Austria*

Email: erich.gnaiger@oroboros.at

Tel: +43 512 566796, Fax: +43 512 566796 20

Abstract

Clarity of concepts and consistency of nomenclature are hallmarks of the quality of a research field across its specializations, aimed at facilitating transdisciplinary communication and education. As mitochondrial physiology continues to expand, the necessity for improved harmonization of nomenclature on mitochondrial respiratory states and rates has become apparent. Peter Mitchell's concept of the protonmotive force establishes the link between electron transfer and phosphorylation of ADP to ATP, and between the electric and chemical components of energy transformation. This unifying concept provides the framework for developing a consistent terminology on mitochondrial physiology and bioenergetics. We follow IUPAC guidelines on general terms of physical chemistry, extended by concepts of open systems and irreversible thermodynamics. The nomenclature of classical bioenergetics on respiratory states 1 to 5 in an experimental protocol is incorporated into a concept-driven constructive terminology to address the meaning of each respiratory state. Hence we focus primarily on the conceptual 'why' with clarification of the experimental 'how'. The capacity of *oxidative phosphorylation*, OXPHOS, provides diagnostic reference values and is, therefore, measured at saturating concentrations of ADP and inorganic phosphate. The contribution of *nonphosphorylating* oxygen consumption is most easily studied by arresting phosphorylation, when oxygen consumption compensates mainly for the proton leak, and the corresponding states are collectively classified as LEAK states. The *oxidative* capacity of the electron transfer system, ETS, reveals the limitation of OXPHOS capacity mediated by the capacity of the *phosphorylation* system. Experimental standards for evaluation of these respiratory coupling states must be followed for the development of databases of mitochondrial respiratory function.

Keywords: Mitochondrial respiratory control, coupling control; mitochondrial preparations, protonmotive force, chemiosmotic theory, oxidative phosphorylation,

efficiency; electron transfer system, ETS; proton leak, LEAK; residual oxygen consumption, ROX; State 2, State 3, State 4.

- * Does the public expect that biologists understand Darwin's theory of evolution?
- * Do students expect that researchers of bioenergetics can explain Mitchell's theory of chemiosmotic energy transformation?

1. Introduction

Every study of mitochondrial function and disease in tissues and cells is faced with evolution, age, gender, lifestyle and environment (EAGLE) as essential background conditions characterizing the individual patient or subject, cohort, species, tissue and even cell line. As a large and highly coordinated group of laboratories and researchers, the global MITOEAGLE network is uniquely poised to generate the necessary scale, type, and quality of consistent data sets to address this intrinsic complexity. The mission of the MITOEAGLE network aims at developing harmonized experimental protocols and implementing a quality control and data management system to interrelate results obtained in different studies and to generate a rigorously monitored database focused on mitochondrial respiratory function.

Reliability and comparability of quantitative results depends on the accuracy of measurement under well-defined conditions. A conceptually meaningful framework is required to relate the results of experiments carried out by different research groups. Vague or ambiguous terminology can lead to confusion and may relegate valuable signals to wasteful noise. For this reason, measured values must be expressed in common units for each well-defined attribute for mitochondrial respiratory control. Standardization of nomenclature and technical jargon is an optimistic goal that can improve the awareness of the intricate meaning of divergent scientific vocabulary. The MITOEAGLE Terminology Group aims at accomplishing the ambitious goal to harmonize, unify and thus simplify the terminology in

the field of mitochondrial physiology. A focus on coupling states in mitochondrial preparations can be considered as a first step in the attempt to generate a harmonized and conceptually oriented nomenclature in bioenergetics and mitochondrial physiology.

Mitochondrial preparations, mtprep, are defined as tissue or cellular preparations in which the plasma membranes are either removed (isolated mitochondria), or mechanically and/or chemically permeabilized (tissue homogenate, permeabilized fibres, permeabilized cells), while mitochondrial functional integrity and to a large extent the mitochondrial structure are maintained.

2. Fundamental respiratory coupling states in mitochondrial preparations

‘Every professional group develops its own technical jargon for talking about matters of critical concern ... People who know a word can share that idea with other members of their group, and a shared vocabulary is part of the glue that holds people together and allows them to create a shared culture’ (Miller 1991).

Mitochondrial respiratory control is exerted in a mitochondrial preparation by experimental conditions defined as respiratory states. Coupling states in mitochondrial preparations depend on the exogenous supply of fuel substrates and oxygen to support the electron transfer system (Fig. 1). The phosphorylation of ADP to ATP is stimulated or depressed which causes an increase or decrease of electron flow linked to oxygen consumption in ‘controlled’ coupling states. Alternatively, coupling of electron transfer with phosphorylation is disengaged by uncouplers, and the corresponding ‘uncontrolled’ state is characterized by high levels of oxygen consumption without performance of biochemical work (Fig. 2). Such uncoupling is different from switching to mitochondrial pathways that involve less than three coupling sites with electron entry into the Q-junction bypassing Complex I (Fig. 1). A bypass of the third coupling site (Complex IV) is provided by alternative oxidases, which reduce oxygen without

proton translocation. Reprogramming mitochondrial pathways may be considered as a switch of gears (stoichiometry) rather than uncoupling (loosening the stoichiometry).

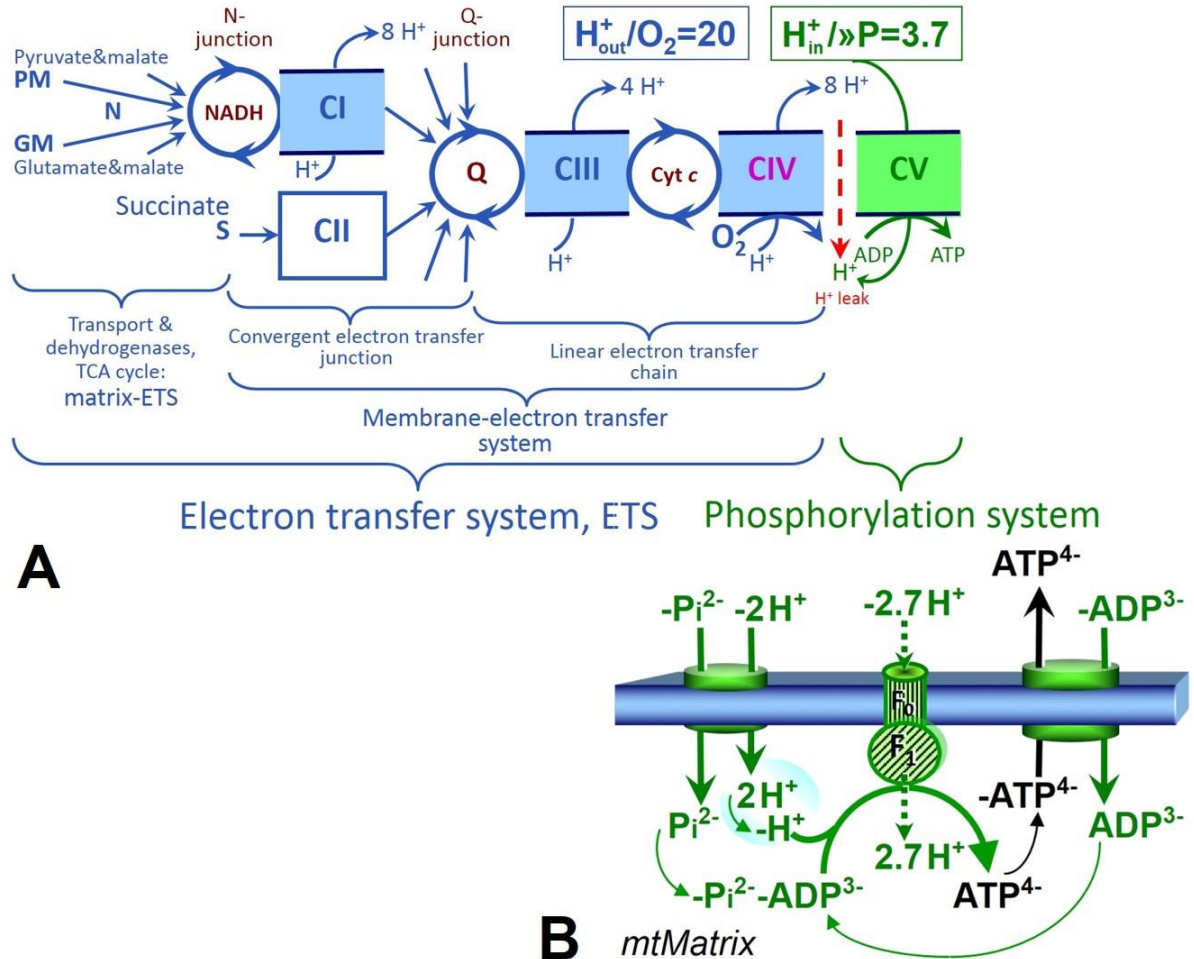


Fig. 1. The mitochondrial respiratory system. In oxidative phosphorylation the electron transfer system (A; to be updated by L Szalov) is coupled to the phosphorylation system (B). See Eqs. 4 and 5 for further explanation. Modified from (A) Lemieux et al. (2017) and (B) Gnaiger (2014).

Phosphorylation, »P: Although *phosphorylation* in the context of OXPHOS is clearly defined as phosphorylation of ADP to ATP, it also potentially involves substrate-level phosphorylation as part of the tricarboxylic acid cycle (succinyl-CoA ligase), in the matrix (phosphoenylpyruvate carboxykinase) and in the cytosol (pyruvate kinase, phosphoglycerate

kinase). ADP is formed in the adenylate kinase reaction, $2 \text{ADP} \leftrightarrow \text{ATP} + \text{AMP}$. In isolated mammalian mitochondria ATP production related to adenylate kinase can be detected in the presence of ADP and without respiratory substrates (Komlódi and Tretter 2017). On the other hand, the term phosphorylation is used in the general literature in many different contexts (phosphorylation of enzymes, etc.). This justifies consideration of a symbol more discriminative than P as used in the P/O ratio (phosphate to atomic oxygen ratio), where P indicates phosphorylation of ADP to ATP or GDP to GTP. We propose the symbol »P for the energetic uphill direction of phosphorylation coupled to catabolic reactions, and likewise the symbol «P for the corresponding downhill reaction (Fig. 2).

Control and regulation: The terms metabolic *control* and *regulation* are frequently used synonymously, but are distinguished in metabolic control analysis (Fell 1997). Respiratory control may be exerted by (1) ATP demand (Fig. 2), (2) fuel substrate, pathway competition and oxygen availability (starvation and hypoxia), (3) the protonmotive force, redox states, flux-force relationships, coupling and efficiency, (4) mitochondrial enzyme activities and allosteric regulation by adenylates, phosphorylation of regulatory enzymes, Ca^{2+} and other ions including H^+ , (5) inhibitors (e.g. NO or intermediary metabolites, such as oxaloacetate), (6) enzyme content, concentrations of cofactors and conserved moieties (such as adenylates, NADH/NAD⁺, coenzyme Q, cytochrome *c*); (7) metabolic channeling by supercomplexes, (8) mitochondrial density and morphology (fission and fusion), (9) hormone levels, gender, life style (influencing all control mechanisms listed before), and (10) genetic or acquired diseases causing mitochondrial dysfunction (for reviews see Brown 1992; Gnaiger 1993a, 2009; 2014; Morrow et al. 2017).

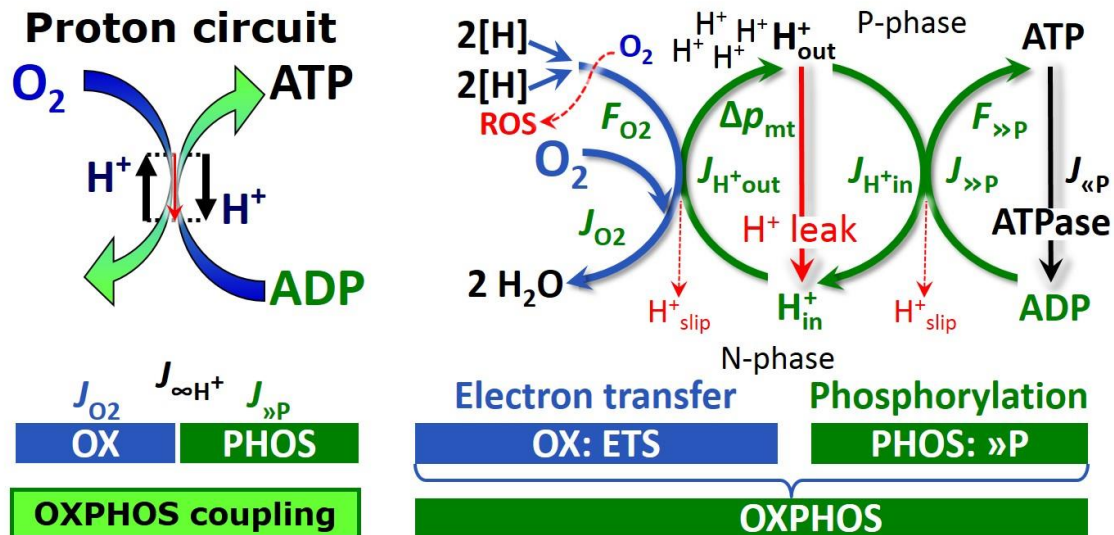


Fig. 2. The proton circuit and coupling in oxidative phosphorylation (OXPHOS). Oxygen flux, J_{O_2} , is coupled to the phosphorylation of ADP to ATP, $J_{\gg P}$, by the proton pumps of the electron transfer system (ETS) pushing the outwards proton flux, J_{H^+out} . The ATP synthase is driven by the protonmotive force, Δp_{mt} , and inwards proton flux, J_{H^+in} , to phosphorylate ADP to ATP. $2[H]$ indicates the reduced hydrogen equivalents of fuel substrates providing the chemical input force or molar Gibbs energy, F_{O_2} [kJ/mol O_2], of the reaction with oxygen, typically in the range of -460 to -480 kJ/mol. The output force is given by the phosphorylation potential, $F_{\gg P}$ [kJ/mol ADP phosphorylated to ATP], which varies *in vivo* in the range of about 48 to 62 kJ/mol under physiological conditions. Proton turnover, $J_{\infty H^+}$, and ATP turnover, $J_{\ll P}$, proceed in the steady state at constant Δp_{mt} , when $J_{\infty H^+} = J_{H^+out} = J_{H^+in}$, and at constant phosphorylation potential, $F_{\gg P}$, when $J_{\ll P} = J_{\gg P} = J_{\ll P}$. $J_{\gg P}/J_{O_2}$ ($\gg P/O_2$) is two times the 'P/O' ratio of classical bioenergetics. The effective $\gg P/O_2$ ratio is diminished by (i) the proton leak across the inner mitochondrial membrane from low pH in the positive P-phase to the negative N-phase, (ii) cycling of other cations, (iii) proton slip of the proton pumps when effectively a proton is not pumped, and (iv) electron leak generating reactive oxygen species, ROS. Modified from Gnaiger (2014).

2.1. Classical terminology for isolated mitochondria

'When a code is familiar enough, it ceases appearing like a code; one forgets that there is a decoding mechanism. The message is identical with its meaning'
(Hofstadter 1979).

Five classical states of mitochondrial respiration and cytochrome redox states were introduced by Chance and Williams (1955; 1956). Table 1 explains a protocol with isolated mitochondria in a closed respirometric chamber, defining a consecutive sequence of respiratory states.

State 1 is obtained after addition of isolated mitochondria to air-saturated isoosmotic/isotonic respiration medium containing inorganic phosphate, but no adenylates (i.e., AMP, ADP, ATP) and no fuel substrates.

State 2 is induced by addition of a high concentration of ADP (typically 100 to 300 μM), which stimulates respiration transiently on the basis of endogenous fuel substrates and phosphorylates only a small portion of the added ADP. State 2 is then obtained at a low respiratory activity limited by endogenous fuel substrate availability.

State 3 is the state stimulated by addition of fuel substrates while the ADP concentration is still high (Table 1) and supports coupled energy transformation in oxidative phosphorylation. 'High ADP' is a concentration of ADP specifically selected to allow the measurement of State 3 to State 4 transitions of isolated mitochondria in a closed respirometric system. A repeated ADP titration re-establishes State 3 at 'high ADP'. Starting at oxygen concentrations near air saturation (ca. 200 μM O_2), the total ADP concentration added must be low enough (typically 100 to 300 μM) to allow phosphorylation to ATP at a coupled oxygen consumption that does not lead to oxygen depletion during the transition to State 4. In contrast, kinetically saturating ADP concentrations are usually an order of magnitude higher than 'high ADP'.

State 4 is only reached if the mitochondrial preparation is of high quality and is well coupled.

Depletion of ADP by phosphorylation to ATP will then lead to a decline in oxygen uptake in the transition from State 3 to State 4. Under these conditions a maximum Δp_{mt} and high ATP/ADP ratio are maintained. State 4 respiration reflects intrinsic proton leak and the ATPase activity.

State 5 is a state obtained after exhaustion of oxygen in a closed respirometric chamber.

Oxygen back-diffusion into the aqueous solution may be a confounding factor preventing complete anoxia (Gnaiger 2001).

Table 1. Metabolic states of mitochondria (after Chance and Williams, 1956).

State	[O ₂]	[ADP]	[Substrate]	Respiration rate	Rate-limiting substance
1	>0	Low	Low	Slow	ADP
2	>0	High	~0	Slow	Substrate
3	>0	High	High	Fast	Respiratory chain
4	>0	Low	High	Slow	ADP
5	0	High	High	0	Oxygen

2.2. Three coupling states of mitochondrial preparations and residual oxygen consumption

It has been suggested to extend the differential nomenclature (States 1 to 5) by a concept-driven terminology carrying explicit information on the nature of the respiratory states (Gnaiger 2009). Coupling states of mitochondrial preparations can be compared in any mitochondrial pathway control state, i.e., keeping fuel substrates and ETS inhibitors constant while varying adenylate levels and inhibitors of the phosphorylation system (Fig. 1). The terminology must be general and not restricted to any particular experimental protocol or mitochondrial preparation.

OXPHOS state (Fig. 3): The

respiratory state with saturating levels of oxygen, respiratory and phosphorylation substrates, and zero uncoupler, to provide an estimate of the maximal capacity of OXPHOS in any given pathway control state. Respiratory capacities at

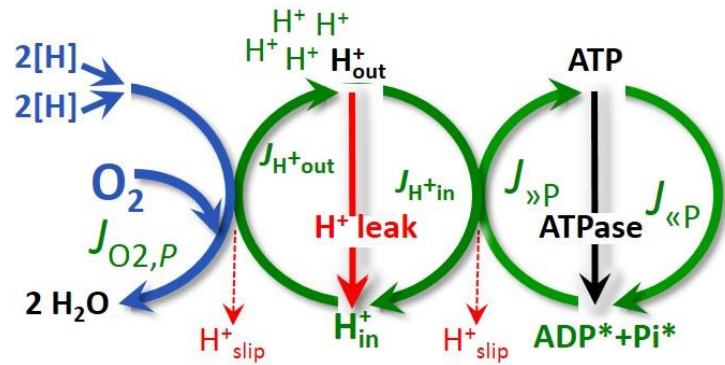


Fig. 3. OXPHOS state when phosphorylation, $J_{>P}$, is supported by a high Δp_{mt} , is stimulated by saturating [ADP]* and inorganic phosphate, [Pi]*. Oxygen flux, $J_{O_2,P}$, is highly coupled at a maximum $\gg P/O_2$ ratio, $J_{>P}/J_{O_2,P}$ (see also Fig. 2).

saturating substrate concentrations provide reference values or upper limits of performance, aiming at the generation of data sets for comparative purposes. Any effects of substrate kinetics are thus separated from reporting actual mitochondrial capacities, against which physiological activities can be evaluated.

As discussed previously, 0.2 mM ADP does not fully saturate flux in isolated mitochondria (Gnaiger 2001; Puchowicz et al. 2004), and even higher ADP concentrations are required, particularly in permeabilized muscle fibres, to overcome limitations by diffusion and by the tubulin-regulated conductance of the outer mitochondrial membrane (Rostovtseva et al. 2008). In permeabilized muscle fibre bundles of high respiratory capacity, the apparent K_m for ADP increases up to 0.5 mM (Saks et al. 1998). This implies that >90 % saturation is reached only at >5 mM ADP.

ETS state (Fig. 4): The electron transfer system state or ETS state is defined as the non-

controlled state with saturating levels of oxygen, respiratory substrate and uncoupler, as an estimate of the maximal capacity of the ETS.

Optimal *exogenous* uncoupler concentration for maximum oxygen flux provides the condition for

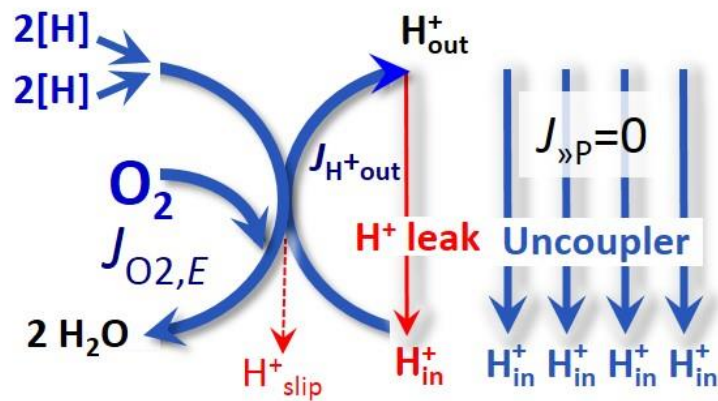


Fig. 4. ETS state when noncoupled respiration, $J_{O_2,E}$, is maximum at optimum exogenous uncoupler concentration and phosphorylation is zero, $J_{\gg P}=0$ (see also Fig. 2).

measurement of ETS capacity. As a consequence of the nearly collapsed Δp_{mt} , the driving force for phosphorylation is missing and $J_{\gg P}=0$. The abbreviation State 3u is used frequently in bioenergetics, to indicate the state of maximum respiration without sufficient emphasis on the fundamental difference between OXPHOS capacity (*well coupled* with an *endogenous* uncoupled component) and ETS capacity (*noncoupled*).

LEAK state (Fig. 5): A state of

mitochondrial respiration when oxygen flux is maintained at saturating levels of oxygen and respiratory substrates, and zero ATP-turnover without addition of any experimental uncoupler, as

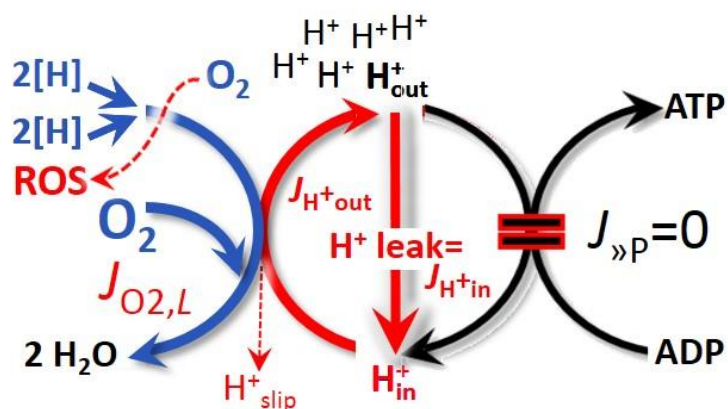


Fig. 5. LEAK state when phosphorylation is arrested, $J_{\gg P}=0$, and oxygen flux, $J_{O_2,L}$, is controlled mainly by the proton leak, which equals J_{H^+in} , at maximum Δp_{mt} (see also Fig. 2).

an estimate of the maximal proton leak rate. The LEAK state can be measured either (i) in the absence of adenylates, (ii) after depletion of ADP at maximum ATP/ADP ratio, or (iii) after inhibition of the phosphorylation system by inhibitors such as oligomycin (ATP synthase) or carboxyatractyloside (adenylate nucleotide translocase). State 4 represents an overestimation of LEAK respiration if the ATPase activity maintains some stimulation of respiration by recycled ADP at $J_{\text{»P}} > 0$. This can be tested by inhibition of the phosphorylation system using oligomycin, ensuring that $J_{\text{»P}} = 0$.

Proton leak: Proton leak is the process in which protons are translocated across the inner mitochondrial membrane in the direction of the downhill protonmotive force without coupling to phosphorylation. The proton leak flux depends on Δp_{mt} and is a property of the inner mitochondrial membrane.

Proton slip: Proton slip is the process in which protons are only partially translocated by a proton pump and slip back to the original compartment. The proton slip is a property of the proton pump and depends on the turnover rate of the proton pump.

ROX: Residual oxygen consumption (ROX) is defined as oxygen consumption due to oxidative side reactions remaining after inhibition of the ETS. ROX is not a coupling state but represents a baseline that is used to correct mitochondrial respiration in defined coupling states. ROX is not necessarily equivalent to non-mitochondrial respiration, considering oxygen-consuming reactions in mitochondria not related to ETS, such as oxygen consumption in the monoamine oxidase catalyzed reaction. In the presence of oxygen, ROX is measured either in the absence of fuel substrates or after blocking the electron supply to cytochrome *c* oxidase and alternative oxidases.

3. States and rates

Fig. 6 summarizes the three coupling states, ETS, LEAK and OXPHOS, and puts them into a schematic context with the corresponding respiratory rates, abbreviated as E , L and P , respectively. This clarifies that E may exceed or be equal to P , but E cannot theoretically be lower than P . $E < P$ must be discounted as an artefact, which may be caused experimentally by (i) using high and inhibitory uncoupler concentrations (Gnaiger 2008), (ii) non-saturating [ADP] or [Pi] (State 3), (iii) high oligomycin concentrations applied for measurement of L before titrations of uncoupler, when oligomycin exerts an inhibitory effect on E , or (iv) loss of oxidative capacity during the time course of the respirometric assay with E measured subsequently to P (Gnaiger 2014). On the other hand, $E > P$ is observed in many types of mitochondria and depends on (i) the excess ETS capacity pushing the phosphorylation system (Fig. 1B) to the limit of its *capacity of utilizing* Δp_{mt} , (ii) the pathway control state with single or multiple electron input into the Q-junction and involvement of three or less coupling sites determining the $\text{H}^+_{\text{out}}/\text{O}_2$ *coupling stoichiometry* (Fig. 2A), and (iii) the *biochemical coupling efficiency* expressed as $(E-L)/E$, since any increase of L causes an increase of P upwards to the limit of E . The *excess E-P capacity*, $ExP = E - P$, therefore, provides a sensitive diagnostic indicator of specific injuries of the phosphorylation system, when E remains constant but P declines relative to controls (Fig. 6). Substrate cocktails supporting simultaneous convergent electron transfer to the Q-junction for reconstitution of TCA cycle function stimulate ETS capacity, and consequently increase the sensitivity of the ExP assay.

When subtracting L from P , the dissipative LEAK component in the OXPHOS state may be overestimated. This can be avoided by measurement of LEAK respiration in a state when the protonmotive force, Δp_{mt} , is adjusted to the slightly lower value maintained in the OXPHOS state. Any turnover-dependent components of proton leak and slip, however, are underestimated under these conditions (Garlid et al. 1993). In general, it is inappropriate to use the term *ATP production* for the difference of oxygen consumption measured in states P

and L . The difference $P-L$ is the upper limit of the part of OXPHOS capacity which is *free* (corrected for LEAK respiration) and is fully coupled to phosphorylation with a maximum mechanistic stoichiometry, $\approx P = P-L$ (Fig. 6).

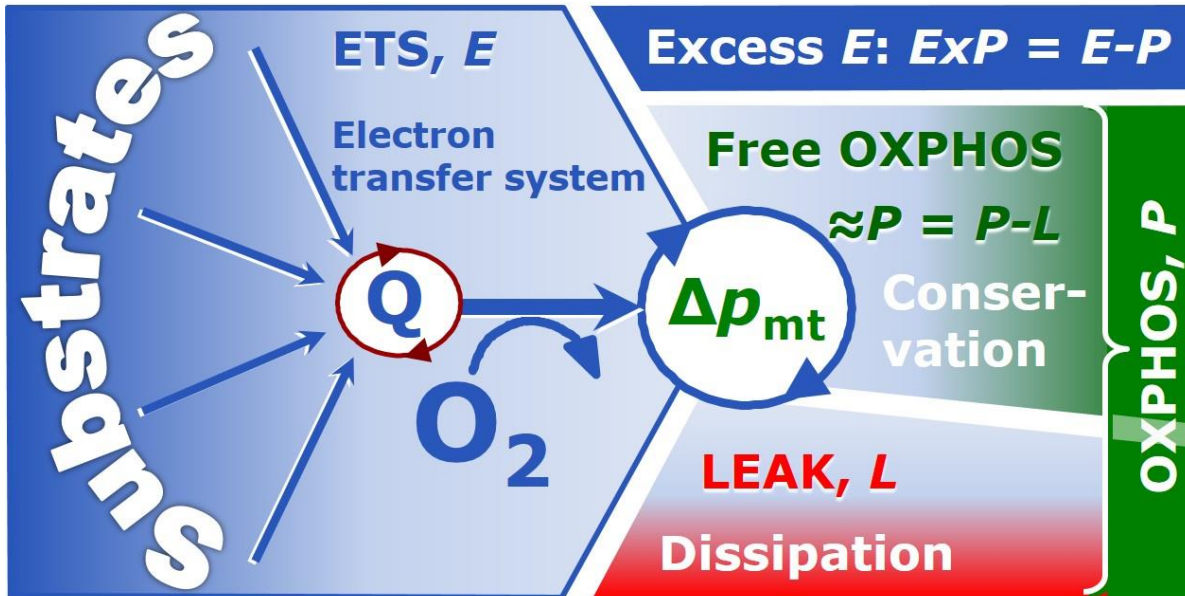


Fig. 6. Four-compartmental model of oxidative phosphorylation with respiratory states (ETS, OXPHOS, LEAK) and corresponding rates (E , P , L). Modified from Gnaiger (2014).

3.1. The steady-state

Steady-state variables (membrane potential; redox states) and metabolic fluxes (*rates*) are measured in defined mitochondrial respiratory *states*. Strictly, steady states can be obtained only in open systems, in which changes due to internal transformations (e.g., oxygen consumption) are instantaneously compensated by external flows (e.g., oxygen supply), such that oxygen concentration does not change in the system (Gnaiger 1993b). Mitochondrial respiratory states monitored in closed systems may satisfy the criteria of pseudo-steady states for limited periods of time, when the changes occurring in the system (concentrations of oxygen, fuel substrates, ADP) do not exert significant effects on metabolic fluxes (respiration, phosphorylation). Such pseudo-steady states require saturating levels of substrates to be maintained and thus depend on the kinetics of the processes under investigation.

Protonmotive force, Δp_{mt} : The protonmotive force, Δp_{mt} ,

$$\Delta p_{mt} = \Delta \Psi_{mt} + \Delta \mu_{H^+} / F \quad (1)$$

is composed of an electric part, $\Delta \Psi_{mt}$, which is the difference of charge (electrical potential difference) across the inner mitochondrial membrane, and a chemical part incorporating the Faraday constant, $\Delta \mu_{H^+}/F$, which stems from the difference of pH (chemical potential difference) across the mitochondrial membrane. Protonmotive means that protons are moved across the mitochondrial membrane at $\Delta p_{H_{mt}}$ maintained across the mt-membrane,

$$\Delta \mu_{H^+} = -\ln(10) \cdot RT \cdot \Delta p_{H_{mt}} \quad (2)$$

where RT is the gas constant times absolute temperature. $\ln(10) \cdot RT = 5.708$ and 5.938 $\text{kJ} \cdot \text{mol}^{-1}$ at 25 and 37 °C, respectively. The Faraday constant, $F = e \cdot N_A$, is the product of the elementary charge, e [C], and the Avogadro (or Loschmidt) constant, N_A . F yields the conversion between electric force, $\Delta \Psi_{mt}$, expressed in joules per *motive* coulomb or volt [$\text{V}=\text{J}/\text{C}$] and chemical force, $\Delta \mu_{H^+}$, with the unit joules per *motive* mole [J/mol]. $\ln(10) \cdot RT/F = 59.16$ and 61.54 mV at 25 and 37 °C, respectively. For a ΔpH of 1 unit, the chemical potential difference (Eq. 2) changes by $6 \text{ kJ} \cdot \text{mol}^{-1}$ and Δp_{mt} (Eq. 1) changes by 0.06 V. Since F equals $96.5 \text{ (kJ} \cdot \text{mol}^{-1})/\text{V}$, a membrane potential of -0.2 V (Eq. 1) equals a chemiosmotic potential difference, $\Delta \tilde{\mu}_{H^+}$, of $19 \text{ kJ} \cdot \text{mol}^{-1} \text{ H}^+_{\text{out}}$. Considering a driving force of $-470 \text{ kJ} \cdot \text{mol}^{-1} \text{ O}_2$ for oxidation, the thermodynamic limit of the $\text{H}^+_{\text{out}}/\text{O}_2$ ratio is reached at a value of $470/19 = 24$, compared to a mechanistic stoichiometry of 20 ($\text{H}^+_{\text{out}}/\text{O}=10$).

The protonmotive force is *elevated* in the LEAK state of coupled mitochondria, driven by LEAK respiration at a minimum back flux of protons to the matrix side. Δp_{mt} is *high* in the OXPHOS state when it drives phosphorylation, and *very low* in the ETS state when uncouplers short-circuit the proton cycle.

Forces and flows in physics and irreversible thermodynamics: According to definition in physics, a potential difference and as such the *protonmotive force*, Δp_{mt} , is not a

force (Cohen et al 2008). The fundamental forces of physics are distinguished from *motive forces* (e.g. Δp_{mt}) of statistical and irreversible thermodynamics. Complementary to the attempt towards unification of fundamental forces defined in physics, the concepts of Nobel laureates Lars Onsager, Erwin Schrödinger, Ilya Prigogine and Peter Mitchell (even if expressed in apparently unrelated terms) unite the diversity of ‘isomorphic’ *flow-force* relationships, the product of which links to the dissipation function and Second Law of thermodynamics (Schrödinger 1944; Prigogine 1967). A *motive force* is the change of potentially available or ‘free’ energy (exergy) per isomorphic *motive* unit (force=exergy/motive unit; in integral form, this definition takes care of isothermal and non-isothermal processes). A potential difference is, in the framework of flow-force relationships, an isomorphic force, F_{tr} , involved in an exergy transformation, defined as the *partial* derivative of Gibbs energy, $\partial_{\text{tr}}G$, per advancement, $\partial_{\text{tr}}\zeta$, of the transformation, tr (the isomorphic motive unit in the transformation): $F_{\text{tr}} = \partial_{\text{tr}}G/\partial_{\text{tr}}\zeta$ (Gnaiger 1993a,b). This formal generalization represents an appreciation of the conceptual beauty of Peter Mitchell’s innovation of the protonmotive force against the background of the established paradigm of the electromotive force (emf) defined at the limit of zero current (Cohen et al. 2008).

Molar quantities: ‘The adjective *molar* before the name of an extensive quantity generally means *divided by amount of substance*’ (Cohen et al 2008). The notion that all molar quantities then become *intensive* causes ambiguity in the meaning of *molar Gibbs energy*. It is important to emphasize the fundamental difference between normalization for *amount of substance* B in a system, where $dn_{\text{B}}/dt \cdot V^{-1}$ is the *rate of concentration change* [$\text{mol} \cdot \text{s}^{-1} \cdot \text{m}^{-3}$], versus normalization for *amount of motive substance*, where $d_{\text{r}}\zeta_{\text{B}}/dt \cdot V^{-1}$ is the volume-specific flux of chemical reaction r. When the Gibbs energy of a system, G [J], is divided by the amount of substance B, n_{B} [mol], a *size-specific* molar quantity is obtained, $G_{\text{m}} = G/n_{\text{B}}$ [$\text{J} \cdot \text{mol}^{-1}$], which is not an (isomorphic) force. In contrast, when the partial Gibbs energy change, $\partial_{\text{r}}G$ [J], is divided by the motive amount of substance B in reaction r

(advancement of reaction), $\partial_r \zeta_B$ [mol], the resulting *intensive* molar quantity, $F_r = \partial_r G / \partial_r \zeta_B$ [$\text{J}\cdot\text{mol}^{-1}$], is the chemical force of reaction r involving 1 mol B (-1 or 1, depending on B being a product or substrate, respectively).

Vectorial and scalar forces and fluxes: In chemical reactions and osmotic or diffusion processes occurring in a closed heterogeneous system, such as a chamber containing isolated mitochondria, scalar transformations occur without measured spatial direction but between separate compartments (translocation between the matrix and intermembrane space) or between energetically separated chemical substances (reactions from substrates to products). Hence the corresponding fluxes are not vectorial but scalar, and are expressed per volume and not per membrane area. The corresponding motive forces are also scalar, expressed in units [$\text{J}\cdot\text{mol}^{-1}$] as potential *differences* across the membrane, without taking into account the *gradients* across the 6 nm thick inner mitochondrial membrane (Rich 1993). In a scalar electric transformation (flux of charge or current from the matrix space to the intermembrane and extramitochondrial space) the motive force is the difference of charge, $\Delta\Psi_{\text{mt}}$ [$\text{V}=\text{J}\cdot\text{C}^{-1}$]. For comparison, in a mechanical, vectorial advancement, $d_{\text{me}}\zeta$ [m], the unit of the *force* is newton, F_{me} [$\text{N}=\text{J}\cdot\text{m}^{-1}$], and *flow* is the velocity, $v = d_{\text{me}}\zeta/dt$ [$\text{m}\cdot\text{s}^{-1}$], such that the flow·force product yields mechanical power, P_{me} [W] (Cohen et al 2008). The corresponding *vectorial flux* (flow density per area) is velocity per cross-sectional area [$\text{s}^{-1}\cdot\text{m}^{-1}$]. The *scalar flux* lacks spatial information in a given volume, such that flux ($\text{m}\cdot\text{s}^{-1}$ per volume [$\text{s}^{-1}\cdot\text{m}^{-2}$]) times force yields volume-specific power, $P_{V\text{me}}$ [$\text{W}\cdot\text{m}^{-3}$].

Coupled versus bound processes: Since the chemiosmotic theory explains the mechanism of coupling in OXPHOS, it may be interesting to ask if the electrical and chemical parts of proton translocation are coupled processes. This is not the case according to the definition of coupling: Coupling occurs in an energy transformation between processes, if a coupling mechanism allows work to be performed on the endergonic or uphill *output* process (work per unit time is power; dW/dt [J/s] = P_{out} [W]; with a positive partial Gibbs energy

change) driven by the exergonic or downhill *input* process (with a negative partial Gibbs energy change). If the coupling mechanism is disengaged, the output process becomes independent of the input process, and both proceed in their downhill direction (Fig. 2). It is not possible to physically uncouple the electrical and chemical processes, which are only *theoretically* partitioned as electrical and chemical components (Eq. 1) and can be measured separately. If partial processes (fluxes, forces) are non-separable, i.e., cannot be uncoupled, then these are not *coupled* but are defined as *bound* processes. The electrical and chemical part of Eq. 1 are tightly bound partial forces of the protonmotive force.

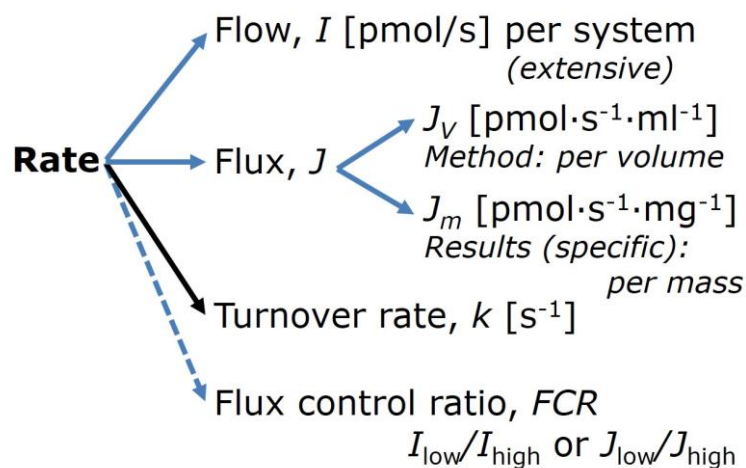
Coupling, efficiency and power: In energetics (ergodynamics) coupling is defined as an exergy transformation fuelled by an exergonic (downhill) input process driving the advancement of an endergonic (uphill) output process. The (negative) output/input power ratio is the efficiency of a coupled energy transformation. Power, $P_{tr} = \partial_{tr}G/dt$ [$W=J\cdot s^{-1}$], is closely linked to the dissipation function (Prigogine 1967) and is the product of flow, $I_{tr}=d_{tr}\xi\cdot dt^{-1}$ [$x_{tr}\cdot s^{-1}$] times generalized force, $F_{tr} = \partial_{tr}G/\partial_{tr}\xi$ [$J\cdot x_{tr}^{-1}$] (Gnaiger 1993b). At the limit of maximum efficiency of a completely coupled system, the (negative) input power equals the (positive) output power, such that the total power equals zero at an efficiency of 1.

3.2. Normalization: flows and fluxes

Application of common and generally defined units is required for direct transfer of reported results into a database. The second [s] is the *SI* unit for the base quantity *time*. Table 2 lists some conversion factors to obtain *SI* units. The term *rate* is too general and not useful for a database (Fig. 7).

Extensive quantities: An extensive quantity increases proportionally with system size. The magnitude of an extensive quantity is completely additive for non-interacting subsystems, such as mass or flow expressed per defined system. The magnitude of these quantities depends on the extent or size of the system (Cohen et al. 2008).

Fig. 7. Different meanings of *rate* may lead to confusion, if the normalization is not sufficiently specified. Results are frequently expressed as mass-specific *flux*, J_m , per mg protein, dry or wet



weight, ignoring the fundamental difference between weight and mass. Cell volume, V_{ce} , or mitochondrial volume, V_{mt} , may be used for normalization (volume-specific flux, $J_{V_{ce}}$ or $J_{V_{mt}}$), which then must be clearly distinguished from flux, J_v , expressed for methodological reasons per volume of the measurement system.

Size-specific quantities: ‘The adjective *specific* before the name of an extensive quantity is often used to mean *divided by mass*’ (Cohen et al. 2008). A mass-specific quantity (e.g., mass-specific flux is flow divided by mass of the system) is independent of the extent of non-interacting homogenous subsystems. Tissue specific quantities are of fundamental interest in comparative mitochondrial physiology, where *specific* refers to the *type* rather than *mass* of the tissue. The term *specific*, therefore, must be clarified further, such that tissue mass-specific (e.g. muscle mass-specific) quantities are defined.

Flow per system, I : In analogy to electric terms, flow as an extensive quantity (I ; per system) is distinguished from flux as a size-specific quantity (J ; per system size) (Fig. 7). Electric current is a flow, I_{el} [$A = C \cdot s^{-1}$], per system (extensive quantity). When dividing this extensive quantity by system size (the cross-sectional area of a wire or area of a membrane), a size-specific quantity is obtained, which is electric flux (electric current density), J_{el} [$A \cdot m^{-2} = C \cdot s^{-1} \cdot m^{-2}$].

Size-specific flux, J : Oxygen flow per muscle increases as muscle mass is increased. Muscle mass-specific oxygen flux should be independent of the size of the tissue sample studied in the instrumental chamber, but volume-specific oxygen flux (per volume of the instrumental chamber, V) should increase in direct proportion to the amount of sample in the chamber. Accurate definition and reference to the *system* is decisive: the experimental system of the muscle, or the instrumental system of the measurement chamber. Volume-specific oxygen flux depends on mass-concentration of the sample in the chamber, but should be independent of chamber volume. If mass-specific oxygen flux is constant and independent of experimental system size (expressed as mass), then there is no interaction between the subsystems. A 1.5 mg and 3.0 mg muscle sample (wet weight) respire at identical mass-specific flux. The complexity changes when whole organisms are studied as experimental models. The well-established scaling law in respiratory physiology reveals a strong interaction of oxygen consumption and individual body mass of an organism, since *basal* metabolic rate (flow) does not increase linearly with body mass, whereas *maximum* mass-specific oxygen flux, $\dot{V}_{O_{2max}}$, or $\dot{V}_{O_{2peak}}$, is constant across a large range of individual body mass (Weibel and Hoppeler 2005). $\dot{V}_{O_{2peak}}$ of human endurance athletes is 60 up to 80 ml $O_2 \cdot \text{min}^{-1} \cdot \text{kg}^{-1}$ body mass, converted to $J_{m,O_{2peak}}$ of 45 to 60 $\text{nmol} \cdot \text{s}^{-1} \cdot \text{g}^{-1}$ (Table 2).

Flux per volume of the instrumental system, J_V : In open systems, external flows (such as oxygen supply) are distinguished from internal transformations (metabolic flow, oxygen consumption). In closed systems, external flows of all substances are zero and oxygen consumption (internal flow), I_{O_2} [$\text{pmol} \cdot \text{s}^{-1}$], causes a decline of the amount of oxygen in the system, n_{O_2} [nmol]. Normalization of these quantities for the volume of the system, V [$\text{ml} = \text{cm}^3$], yields volume-specific oxygen flux, $J_{V,O_2} = I_{O_2}/V$ [$\text{pmol} \cdot \text{s}^{-1} \cdot \text{ml}^{-1}$], and oxygen concentration, $[O_2]$ or $c_{O_2} = n_{O_2}/V$ [$\text{nmol} \cdot \text{ml}^{-1} = \mu\text{mol} \cdot \text{l}^{-1} = \mu\text{M}$]. Volume-specific metabolic oxygen flux, J_{V,O_2} , depends on the specific activity and the concentration of the mitochondrial preparation in the measurement system, mtprep/V .

Instrumental volume-specific flux, J_{V,O_2} , should be compared with instrumental resolution and is thus relevant mainly for methodological reasons. Normalization for sample concentration, mt_{prep}/V , is required for reporting respiratory results, e.g., in terms of respiration per mass, $W_{mt_{prep}}$ (of tissue homogenate or permeabilized fibres, or mitochondrial protein), $J_{O_2} = J_{V,O_2}/(W_{mt_{prep}}/V) = I_{O_2}/W_{mt_{prep}}$.

Flow per experimental model, I: A special case of normalization is encountered in respiratory studies with permeabilized (or intact) cells. If respiration is expressed per million cells, the oxygen flow per measurement system is replaced by the oxygen flow, I_{O_2} , per cell (or per 10^6 cells). Similarly, oxygen flow can be calculated from volume-specific oxygen flux, J_{V,O_2} [$\text{pmol}\cdot\text{s}^{-1}\cdot\text{ml}^{-1}$] (per V of the measurement chamber), divided by the number density of cells, $C=N_{ce}/V$ [$10^6\cdot\text{ml}^{-1}$], where N_{ce} is the number of cells in the chamber. Cellular oxygen flow can be compared only between cells of identical cell size. Therefore, further normalization is important to obtain cell size-specific oxygen flux or mitochondrial marker-specific oxygen flux (Renner et al. 2003).

Table 2. Conversion of various units used in respirometry and ergometry.

1 Unit	x	Multiplication factor	=	SI-Unit
$\text{pmol}\cdot\text{s}^{-1}$		0.09649		μA
$\mu\text{A} = \mu\text{C}\cdot\text{s}^{-1}$		10.36		$\text{pmol}\cdot\text{s}^{-1}$
$\text{pg}\cdot\text{atom O}\cdot\text{s}^{-1}$		0.5		$\text{pmol O}_2\cdot\text{s}^{-1}$
$\text{ng}\cdot\text{atom O}\cdot\text{min}^{-1}$		8.33		$\text{pmol O}_2\cdot\text{s}^{-1}$
$\text{natom O}\cdot\text{min}^{-1}$		8.33		$\text{pmol O}_2\cdot\text{s}^{-1}$
$\text{nmol O}_2\cdot\text{min}^{-1}$		16.67		$\text{pmol O}_2\cdot\text{s}^{-1}$
$\text{nmol O}_2\cdot\text{min}^{-1}$		16.67		$\text{pmol O}_2\cdot\text{s}^{-1}$
$\text{nmol O}_2\cdot\text{h}^{-1}$		0.2778		$\text{pmol O}_2\cdot\text{s}^{-1}$
$\text{ml O}_2\cdot\text{min}^{-1}$ at STPD		0.744		$\mu\text{mol O}_2\cdot\text{s}^{-1}$
$W = \text{J/s}$ at -470 kJ/mol O_2		-2.128		$\mu\text{mol O}_2\cdot\text{s}^{-1}$

3.3. Conversion: oxygen, protons, ATP

J_{O_2} is coupled in mitochondrial steady states to proton cycling, $J_{\infty H^+} = J_{H^+out} = J_{H^+in}$ (Fig. 2). J_{H^+out} and J_{H^+in} [$\text{pmol}\cdot\text{s}^{-1}\cdot\text{ml}^{-1}$] are converted into an electric flux (per volume), J_{el} [$\mu\text{C}\cdot\text{s}^{-1}\cdot\text{ml}^{-1}=\mu\text{A}\cdot\text{ml}^{-1}$] = J_{H^+out} [$\text{pmol}\cdot\text{s}^{-1}\cdot\text{ml}^{-1}$] $\cdot F$ [$\text{C}\cdot\text{mol}^{-1}$] $\cdot 10^{-6}$. F is the Faraday constant (96,485.3 $\text{C}\cdot\text{mol}^{-1}$; Table 2). At a J_{H^+out}/J_{O_2} ratio or H^+_{out}/O_2 of 20 ($H^+_{out}/O=10$), a volume-specific oxygen flux of $100 \text{ pmol}\cdot\text{s}^{-1}\cdot\text{ml}^{-1}$ would correspond to a proton flux of 2,000 $\text{pmol}\cdot\text{s}^{-1}\cdot\text{ml}^{-1}$ or volume-specific current of $193 \mu\text{A}\cdot\text{ml}^{-1}$.

$$J_{el} [\mu\text{A}\cdot\text{ml}^{-1}] = J_{H^+out} \cdot F \cdot 10^{-6} [\text{pmol}\cdot\text{s}^{-1}\cdot\text{ml}^{-1} \cdot \mu\text{C}\cdot\text{pmol}^{-1}] \quad (3.1)$$

$$J_{el} [\mu\text{A}\cdot\text{ml}^{-1}] = J_{V,O_2} \cdot (H^+_{out}/O_2) \cdot F \cdot 10^{-6} [\mu\text{C}\cdot\text{s}^{-1}\cdot\text{ml}^{-1}=\mu\text{A}\cdot\text{ml}^{-1}] \quad (3.2)$$

ETS capacity in various human cell types including HEK 293, primary HUVEC and fibroblasts ranges from 50 to $180 \text{ pmol}\cdot\text{s}^{-1}\cdot 10^{-6}$ cells (see Gnaiger 2014). At $100 \text{ pmol}\cdot\text{s}^{-1}\cdot 10^{-6}$ cells corrected for ROX (corresponding to a catabolic power of $-48 \mu\text{W}\cdot 10^{-6}$ cells), the current across the mt-membranes, I_{el} , approximates $193 \mu\text{A}\cdot 10^{-6}$ cells or 0.2 nA per cell. See Rich (2003) for an extension of quantitative bioenergetics from the molecular to the human scale, with a transmembrane proton flux equivalent to 520 A in an adult at a catabolic power of -110 W.

For NADH- and succinate-linked respiration, the mechanistic $\gg P/O_2$ ratio (referring to the full 4 electron reduction of O_2) is calculated at $20/3.7$ and $12/3.7$ (Eq. 2) equal to 5.4 and 3.3. The classical $\gg P/O$ ratios (referring to the 2 electron reduction of $0.5 O_2$) are 2.7 and 1.6 (Watt et al. 2010), in direct agreement with the measured $\gg P/O$ ratio for succinate of 1.58 ± 0.02 (Gnaiger et al. 2000; for detailed reviews see Wikström and Hummer 2012; Sazanov 2015),

$$\gg P/O_2 = (H^+_{out}/O_2)/(H^+_{in}/\gg P) \quad (4)$$

In summary (Fig. 1),

$$J_{V,\gg P} [\text{pmol}\cdot\text{s}^{-1}\cdot\text{ml}^{-1}] = J_{V,O_2} \cdot (H^+_{out}/O_2)/(H^+_{in}/\gg P) \quad (5.1)$$

$$J_{V,\gg P} [\text{pmol}\cdot\text{s}^{-1}\cdot\text{ml}^{-1}] = J_{V,O_2} \cdot (\gg P/O_2) \quad (5.2)$$

Considering isolated mitochondria as powerhouses and proton pumps as molecular machines and relating the experimental results to energy metabolism of the intact cell, the cellular »P/O₂ based on oxidation of glycogen is increased by the glycolytic substrate-level phosphorylation of 3 »P/Glyc. Addition the equivalent of 0.5 to the mitochondrial »P/O₂ ratio of 5.4 yields a bioenergetic cell physiological »P/O₂ ratio close to 6. Two NADH equivalents are formed during glycolysis and transported from the cytosol into the mitochondrial matrix, the energetic cost of which must potentially be taken into account. Taking also into account the substrate-level phosphorylation in the TCA cycle, this high »P/O₂ ratio not only reflects proton translocation and OXPHOS studied in isolation, but integrates mitochondrial physiology with energy transformation in the living cell (Gnaiger 1993b).

4. Conclusions

MITOEAGLE can serve as a gateway to better diagnose mitochondrial respiratory defects, which are linked to genetic variations, age-related health risks, gender-specific mitochondrial performance, life style with its consequences on degenerative diseases, and environmental exposure to toxicological agents. The present recommendations on coupling control (Part 1) will be extended to pathway control of mitochondrial respiration (Part 2), substrate-uncoupler-inhibitor-titration (SUIT) protocols and the harmonization of experimental procedures.

To provide an overall perspective of mitochondrial physiology we may link cellular bioenergetics to systemic human respiratory activity, without yet addressing cell- and tissue-specific mitochondrial function. A routine O₂ flow of 234 μmol·s⁻¹ per individual or flux of 3.3 nmol·s⁻¹·g⁻¹ body mass corresponds to -110 W catabolic energy flow at a body mass of 70 kg and -470 kJ/mol O₂. Considering a cell count of 514·10⁶ cells per g tissue mass and an estimate of 300 mitochondria per cell (Ahluwalia 2017), the average oxygen flow per million cells at $J_{m,O_2\text{peak}}$ of 45 nmol·s⁻¹·g⁻¹ (60 ml O₂·min⁻¹·kg⁻¹) is 88 pmol·s⁻¹·10⁻⁶ cells, which

compares well with OXPHOS capacity of human fibroblasts (not ETS but the lower OXPHOS capacity is used as a reference; Gnaiger 2014). We can describe our body as the sum of $36 \cdot 10^{12}$ cells (36 trillion cells). Mitochondrial fitness of our $11 \cdot 10^{15}$ mitochondria (11 quadrillion mt) is indicated if O_2 flow of $0.02 \text{ pmol} \cdot \text{s}^{-1} \cdot 10^{-6} \text{ mt}$ at rest can be activated to $0.3 \text{ pmol} \cdot \text{s}^{-1} \cdot 10^{-6} \text{ mt}$ at high ergometric performance.

Mitochondria, mt: (Greek mitos: thread; chondros: granule) are small organelles of eukaryotic cells with a double membrane separating the intermembrane space and the matrix with tubular or disk-shaped cristae. Mitochondria maintain their nucleus-independent mtDNA and function as powerhouses and chemiosmotic generators in cell respiration or oxidative phosphorylation. Abbreviation: mt, as generally used in mtDNA. Mitochondrion is singular and mitochondria is plural. Mitochondria contain the cytochrome system and ATP synthase or alternative oxidases, the enzymes of the tricarboxylic acid cycle with several dehydrogenases, fatty acid oxidation, and ion transporters including proton pumps in particular. Mitochondria are the oxygen consuming organelles, where the reduction of O_2 is chemiosmotically coupled to conservation of energy in the form of ATP (oxidative phosphorylation; OXPHOS). Mitochondria are partially independent organelles, yet there is a constant crosstalk between them and the cell. Most of their proteins are encoded by the nuclear DNA, and different cellular signaling pathways, such as Ca^{2+} and protein kinases, modulate mitochondrial activity and structure. In addition, mitochondria interact with each other by fusion and fission all affecting their activity and cell respiration. The bioblasts of Richard Altmann (1894) are not only the mitochondria as presently defined, but include symbiotic and free-living bacteria. “For the physiologist, mitochondria afforded the first opportunity for an experimental approach to structure-function relationships, in particular those involved in active transport, vectorial metabolism, and metabolic control mechanisms on a subcellular level” (Ernster and Schatz 1981).

References (*incomplete; www links will be deleted in the final version*)

Ahluwalia A. Allometric scaling in-vitro. Sci Rep 2017;7:42113.

Altmann R. Die Elementarorganismen und ihre Beziehungen zu den Zellen. Zweite vermehrte

Auflage. Verlag Von Veit & Comp, Leipzig 1894;160 pp. -

www.mitoeagle.org/index.php/Altmann_1894_Verlag_Von_Veit_%26_Comp

Brown GC. Control of respiration and ATP synthesis in mammalian mitochondria and cells.

Biochem J 1992;284:1-13. - www.mitoeagle.org/index.php/Brown_1992_Biochem_J

Chance B, Williams GR. Respiratory enzymes in oxidative phosphorylation: III. The steady state. J Biol Chem 1955;217:409-27. -

www.mitoeagle.org/index.php/Chance_1955_J_Biol_Chem-III

Chance B, Williams GR. Respiratory enzymes in oxidative phosphorylation. IV. The respiratory chain. J Biol Chem 1955;217:429-38. -

www.mitoeagle.org/index.php/Chance_1955_J_Biol_Chem-IV

Chance B, Williams GR. The respiratory chain and oxidative phosphorylation. Adv Enzymol Relat Subj Biochem 1956;17:65-134. -

www.mitoeagle.org/index.php/Chance_1956_Adv_Enzymol_Relat_Subj_Biochem

Cohen ER, Cvitas T, Frey JG, Holmström B, Kuchitsu K, Marquardt R, Mills I, Pavese F, Quack M, Stohner J, Strauss HL, Takami M, Thor HL. Quantities, Units and Symbols in Physical Chemistry, IUPAC Green Book 2008;3rd Edition, 2nd Printing, IUPAC & RSC Publishing, Cambridge. -

www.mitoeagle.org/index.php/Cohen_2008_IUPAC_Green_Book

Ernster L, Schatz G Mitochondria: a historical review. J Cell Biol 1981;91:227s-55s. -

www.mitoeagle.org/index.php/Ernster_1981_J_Cell_Biol

Estabrook RW. Mitochondrial respiratory control and the polarographic measurement of ADP:O ratios. Methods Enzymol 1967;10:41-7. -

www.mitoeagle.org/index.php/Estabrook_1967_Methods_Enzymol

Fell D. Understanding the control of metabolism. Portland Press 1997.

Garlid KD, Semrad C, Zinchenko V. Does redox slip contribute significantly to mitochondrial respiration? In: Schuster S, Rigoulet M, Ouhabi R, Mazat J-P (eds) Modern trends in biothermokinetics. Plenum Press, New York, London 1993;287-93.

Gnaiger E. Efficiency and power strategies under hypoxia. Is low efficiency at high glycolytic ATP production a paradox? In: Surviving Hypoxia: Mechanisms of Control and Adaptation. Hochachka PW, Lutz PL, Sick T, Rosenthal M, Van den Thillart G (eds.) CRC Press, Boca Raton, Ann Arbor, London, Tokyo 1993a:77-109. -

www.mitoeagle.org/index.php/Gnaiger_1993_Hypoxia

Gnaiger E. Nonequilibrium thermodynamics of energy transformations. Pure Appl Chem 1993b;65:1983-2002. - www.mitoeagle.org/index.php/Gnaiger_1993_Pure_Appl_Chem

Gnaiger E. Bioenergetics at low oxygen: dependence of respiration and phosphorylation on oxygen and adenosine diphosphate supply. Respir Physiol 2001;128:277-97. -

www.mitoeagle.org/index.php/Gnaiger_2001_Respir_Physiol

Gnaiger E. Mitochondrial pathways and respiratory control. An introduction to OXPHOS analysis. 4th ed. Mitochondr Physiol Network 2014;19.12. Oroboros MiPNet Publications, Innsbruck:80 pp. -

www.mitoeagle.org/index.php/Gnaiger_2014_MitoPathways

Gnaiger E. Capacity of oxidative phosphorylation in human skeletal muscle. New perspectives of mitochondrial physiology. Int J Biochem Cell Biol 2009;41:1837-45. -

www.mitoeagle.org/index.php/Gnaiger_2009_Int_J_Biochem_Cell_Biol

Gnaiger E, Méndez G, Hand SC. High phosphorylation efficiency and depression of uncoupled respiration in mitochondria under hypoxia. Proc Natl Acad Sci USA 2000;97:11080-5. -

www.mitoeagle.org/index.php/Gnaiger_2000_Proc_Natl_Acad_Sci_U_S_A

Hofstadter DR. Gödel, Escher, Bach: An eternal golden braid. A metaphorical fugue on minds and machines in the spirit of Lewis Carroll. Harvester Press 1979;499 pp. -

www.mitoeagle.org/index.php/Hofstadter_1979_Harvester_Press

Komlódi T, Tretter L. Methylene blue stimulates substrate-level phosphorylation catalysed by succinyl-CoA ligase in the citric acid cycle. Neuropharmacology 2017;123:287-98. -

www.mitoeagle.org/index.php/Komlodi_2017_Neuropharmacology

Lemieux H, Blier PU, Gnaiger E. Remodeling pathway control of mitochondrial respiratory capacity by temperature in mouse heart: electron flow through the Q-junction in permeabilized fibers. Sci Rep 2017;7:2840. -

www.mitoeagle.org/index.php/Lemieux_2017_Sci_Rep

Miller GA. The science of words. Scientific American Library New York 1991;276 pp. -

www.mitoeagle.org/index.php/Miller_1991_Scientific_American_Library

Mitchell P, Moyle J. Respiration-driven proton translocation in rat liver mitochondria. Biochem J 1967;105:1147-62. -

www.mitoeagle.org/index.php/Mitchell_1967_Biochem_J

Morrow RM, Picard M, Derbeneva O, Leipzig J, McManus MJ, Gousspillou G, Barbat-Artigas S, Dos Santos C, Hepple RT, Murdock DG, Wallace DC. Mitochondrial energy deficiency leads to hyperproliferation of skeletal muscle mitochondria and enhanced insulin sensitivity. Proc Natl Acad Sci U S A 2017;114:2705-10. -

www.mitoeagle.org/index.php/Morrow_2017_Proc_Natl_Acad_Sci_U_S_A

Prigogine I. Introduction to thermodynamics of irreversible processes. Interscience, New York, 1967;3rd ed.

Puchowicz MA, Varnes ME, Cohen BH, Friedman NR, Kerr DS, Hoppel CL. Oxidative phosphorylation analysis: assessing the integrated functional activity of human skeletal muscle mitochondria – case studies. Mitochondrion 2004;4:377-85. -

www.mitoeagle.org/index.php/Puchowicz_2004_Mitochondrion

- Renner K, Amberger A, Konwalinka G, Gnaiger E. Changes of mitochondrial respiration, mitochondrial content and cell size after induction of apoptosis in leukemia cells. *Biochim Biophys Acta* 2003;1642:115-23. -
www.mitoeagle.org/index.php/Renner_2003_Biochim_Biophys_Acta
- Rich P. Chemiosmotic coupling: The cost of living. *Nature* 2003;421:583. -
www.mitoeagle.org/index.php/Rich_2003_Nature
- Rostovtseva TK, Sheldon KL, Hassanzadeh E, Monge C, Saks V, Bezrukov SM, Sackett DL. Tubulin binding blocks mitochondrial voltage-dependent anion channel and regulates respiration. *Proc Natl Acad Sci USA* 2008;105:18746-51. -
www.mitoeagle.org/index.php/Rostovtseva_2008_Proc_Natl_Acad_Sci_U_S_A
- Rustin P, Parfait B, Chretien D, Bourgeron T, Djouadi F, Bastin J, Rötig A, Munnich A. Fluxes of nicotinamide adenine dinucleotides through mitochondrial membranes in human cultured cells. *J Biol Chem* 1996;271:14785-90.
- Sazanov LA. A giant molecular proton pump: structure and mechanism of respiratory complex I. *Nat Rev Mol Cell Biol* 2015;16:375-88. -
www.mitoeagle.org/index.php/Sazanov_2015_Nat_Rev_Mol_Cell_Biol
- Schrödinger E. What is life? The physical aspect of the living cell. Cambridge Univ Press, 1944. - www.mitoeagle.org/index.php/Gnaiger_1994_BTK
- Watt IN, Montgomery MG, Runswick MJ, Leslie AG, Walker JE. Bioenergetic cost of making an adenosine triphosphate molecule in animal mitochondria. *Proc Natl Acad Sci U S A* 2010;107:16823-7. -
www.mitoeagle.org/index.php/Watt_2010_Proc_Natl_Acad_Sci_U_S_A
- Weibel ER, Hoppeler H. Exercise-induced maximal metabolic rate scales with muscle aerobic capacity. *J Exp Biol* 2005;208:1635-44.

Wikström M, Hummer G. Stoichiometry of proton translocation by respiratory complex I and its mechanistic implications. Proc Natl Acad Sci U S A 2012;109:4431-6. -

www.mitoeagle.org/index.php/Wikstroem_2012_Proc_Natl_Acad_Sci_U_S_A